Cyclic Nonlinear Analysis of Large-Scale Finite Element Meshes Through the Use of Hybrid Modeling (HYMOD)

George Markou, Christos Mourlas and Manolis Papadrakakis

***Abstract*—** The simulation of multistory reinforced concrete structures through the use of 3D detail modeling approaches that account for cracking through the smeared crack approach, under ultimate limit state cyclic loading conditions, is currently an approach that is not available in any research or commercial software, due to the excessive computational demand that rises when dealing with this type of large-scale numerical models. Through this research work, the numerical results that were obtained through the use of the simplified hybrid modeling (HYMOD) approach are presented. HYMOD is used herein to illustrate the capabilities of the method in capturing the experimental results of a full-scale 4-storey RC building that was retrofitted with infill walls and carbon fiber polymer jacketing. The adopted modeling approach was found to be able to have a superior computational performance, thus being able to solve the at hand problem thousands of times in an affordable computational time. It is demonstrated that this type of analysis can provide with the ability to study the cyclic mechanical behavior of full-scale structures under ultimate limit state loading conditions, whereas will further utilize scientists to perform parametric investigations towards the optimum retrofitting design of RC structures at a large-scale numerical level.

***Keywords*—** Hybrid Finite Elements, Cyclic Loading, Retrofitting Walls, Large-Scale Numerical Problems.

I. Introduction

Dealing with the modeling of reinforced concrete (RC) structures under extreme cyclic loading conditions has many numerical challenges given the complexity of the mechanical behavior of the concrete material when cracking occurs. In the last three decades, researchers tried to develop different numerical models that would provide the ability of accurate and computationally efficient simulations. The accuracy limitations of 1D and 2D numerical models is well documented thus researchers turned towards more detailed 3D approaches [1-7] in an attempt to develop accurate and objective modeling methods that will be able to predict the mechanical response of any RC structural member or structure. These research studies foresaw the use of solid elements (8-, 20- and 27-noded hexahedral finite elements) that model the crack openings through the use of the smeared crack approach and model rebars as embedded rod or beam finite elements (FE). Research studies found in the international literature that used this numerical modeling approach for the analysis of the cyclic mechanical response of RC structures, were limited to the study of single RC structural members or relatively small structural configurations (i.e. 1-span RC frame with 1 or 2 storeys).

In order to overcome the computational limitations that arise when using solid FEs, several scientists proposed the use of hybrid models that foresee the combination of different in dimensionality finite elements that discretize the frame of any moment frame. Markou and Papadrakakis [8] presented their findings of a literature review performed on mixed element formulations and other hybrid techniques that were proposed through several publications [9-22], where it was found that only one of them attempted to deal with the nonlinear cyclic analysis of RC frames [19]. As it was reported by Mata et al. [19], they used two different FE models (3D solid and 1D beam elements), where the structure was initially discretized only by using beam finite elements. When predefined regions of the frame entered the nonlinear state, they were assumed as prismatic and were discretized with 3D solid elements so as to compute the updated stiffness matrix and the internal stresses. Then through the use of special transformation procedure, the updated stiffness was send back to the beam model. Due to the increased computational demand [20], the authors had to deployed a parallel solver that was used during the dynamic analysis of their numerical model.

The most recent research work that uses the HYMOD approach was presented in [8] and has set the foundations for the full-scale RC structure simulations by presenting an integrated algorithm that uses 8-noded hexahedral finite elements that treat cracking through the smeared crack approach and model the reinforcement through the use of embedded rebar finite elements (rod or beam). In this work [8], it was shown that a direct discretization of the frame through solid and beam elements has the ability to capture the overall mechanical behavior of RC structures, while maintaining a high accuracy and computational efficiency.

The proposed HYMOD algorithm, which in integrated is Reconan FEA [23] research software, is used herein in

G. Markou is an Associate Professor at the Civil Engineering Department of the UCSC, Concepcion, Alonso de Ribera 2850, Concepcion, Chile (corresponding author to provide phone: +56 41 234 5356; e-mail: markou@ucsc.cl).

Christos Mourlas is a Ph.D. candidate at the Civil Engineering Department of the National Technical University of Athens.

Manolis Papadrakakis is a Professor at the Civil Engineering Department of the National Technical University of Athens.

modeling the loading history test imposed on a 4-storey RC building that was experimentally tested by Martin et. al [24]. The computational efficiency, numerical robustness and accuracy of the proposed algorithm that derived from the numerical investigation will be presented in this paper. Furthermore, the algorithm's ability in capturing the mechanical behavior of retrofitted RC structures is also demonstrated by comparing the experimentally and numerically obtained results.

II. Material Modeling

The adopted HYMOD approach [8] considers two different in dimensionality FE models for discretizing the frame of any building-like structure. These elements are the isoparametric hexahedral element and the Natural Beam-Column Flexibility-Based (NBCFB) fiber element. Given that two FEs of different dimensionality are combined in this case, two concrete material models are considered in order to simulate the under study multi-storey RC structure. For the case of the 1D model, the HYMOD foresees the division of each beam-column section into fibers that have the ability to account for

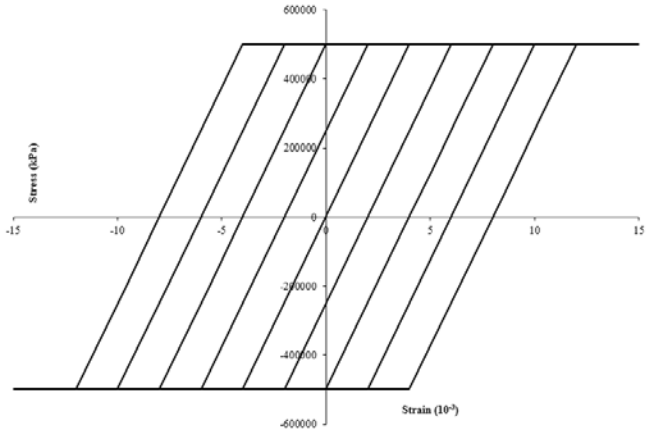

Fig. 1 Bilinear model for cyclic analysis

nonlinearities through the bilinear model (see Fig. 1).

For the case of the 3D concrete material model the constitutive model presented in [6] is adopted for the needs of this work. The model is based on the Kotsovos and Pavlovic [25] material model, whereas it is also integrated with a flexible crack closure criterion that induces numerical stability during the cyclic analysis as it was shown in [6]. According to the formulation of the 3D concrete material constitutive model, the smeared crack approach is used to simulate the crack openings. The smeared crack approach was first presented by Rashid [26] as an extension to the work published by Gonzalez-Vidosa et al. [27]. Through this numerical approach, crack openings are accounted for by modifying the stiffness matrices and stresses at the corresponding integration points (Fig. 2), where the need for remeshing is not required.

For the needs of this research work, the unified total crack approach (UTCA) proposed by Lykidis and Spiliopoulos [2] is adopted, which foresees that the state of crack formation or

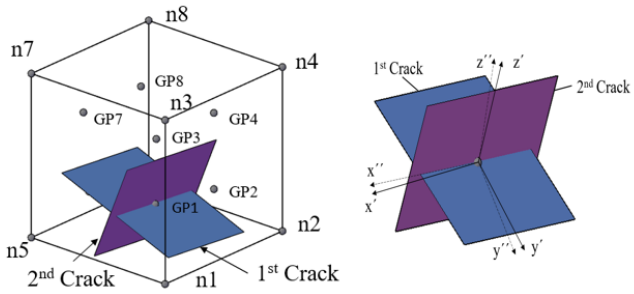

Fig. 2 Local axes for the case of two cracks at a specific Gauss point.

closure is treated in a unified way within every Newton-Raphson internal iteration. The concrete material assumes that it loses all of its carrying capacity along the vertical direction of the crack, thus behaves in a brittle manner. The expression of the strength envelope of concrete is provided in Eq. (1) and it's based on the Willam and Warkne [26] formulae.

$$\tau_{0u}=\frac{2\tau_{0c}(\tau_{0c}^2-\tau_{0e}^2)\cos\theta+\tau_{0c}(2\tau_{0e}-\tau_{0c})\sqrt{4(\tau_{0c}^2-\tau_{0e}^2)\cos^2\theta+5\tau_{0e}^2-4\tau_{0c}^2\tau_{0e}^2}}{4(\tau_{0c}^2-\tau_{0e}^2)\cos^2\theta+(2\tau_{0e}-\tau_{0c})^2} \quad (1)$$

where the rotational variable θ defines the deviatoric stress orientation on the octahedral plane. The τ_{0e} ($\theta=0°$) and τ_{0c} ($\theta=60°$) correspond to the state of $\sigma_1=\sigma_2>\sigma_3$ (triaxial extension) and $\sigma_1>\sigma_2=\sigma_3$ (triaxial compression), respectively and expressed analytically by experimental data.

As it was stated above, the proposed material modeling procedure uses a flexible crack-closing criterion that was proposed in [6], which was found to be crucial during the cyclic loading analysis for establishing faster convergence ratio. The criterion for the closure of cracks is expressed as follows:

$$\varepsilon_i \le \left(b-\frac{n_{cr}-1}{n_{tot}}\right)\varepsilon_{cr} \quad (2)$$

where ε_i is the current strain in the i-direction which is normal to the crack plane and ε_{cr} is the strain that causes cracking formation. Parameter b is the number of the imposed displacement branch of the load history (i.e. Fig. 3 shows 2 imposed displacement branches; equal to a half loading cycle), n_{cr} and n_{tot} are the numbers of increment that the crack is formed at and the total number of increments that an imposed displacement branch is divided into, respectively. Fig. 3

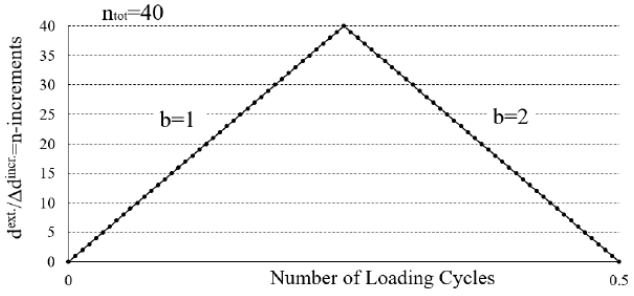

Fig. 3 Schematic representation of the variables of Eq. (2) in an example of a half loading cycle.

illustrates the case where two branches are divided into 40 displacement increments each. The y-axis consists the number of increments (d^{incr} is the imposed displacement of each incremental iteration) and the x-axis represents the number of loading cycles.

When a crack closes at the i-Newton-Raphson iteration, the elastic constitutive matrix D_{el} is used to calculate the stresses of the previously cracked Gauss point through the following expression:

$$\sigma^i = \sigma^{i-1} + D_{el}\Delta\varepsilon^i \tag{3}$$

For the case of the embedded rebar elements found within the hexahedral mesh, the Menegotto-Pinto [29] steel model that takes into account the Bauschinger effect is used. In addition, a full bond model is assumed between the embedded rebars and concrete that complies with the experimental findings [24], which did not report any pull-out failures or insufficient anchorage lengths.

The under study multi-storey RC structure that is investigated in this work, was also retrofitted at the ground floor walls through the use of three-sided Carbon Fiber Reinforced Polymer (CFRP) jackets. In order to account the additional confinement of concrete, the jacketing was also discretized in detail by using hexahedral elements, where the material model used to simulate the stress-strain relationship of the CFRP material foresaw a linear behavior until complete failure for both tension and compression states, as illustrated in Fig. 4. Parameter ρ_c (the compressive-to-tensile strength ratio) was set to 0.7, given that the project's report [24] did not provide any material data in regards to the CFRP sheet that

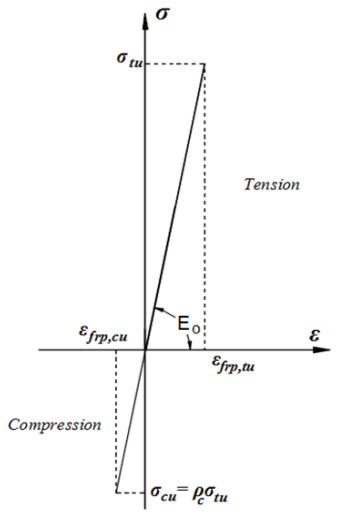

Fig. 4 Material model of the CFRP jacketing. [28]

was used.

III. Hybrid Modeling Formulation

Based on the HYMOD approach, as it was presented in [8] and integrated in this work with the concrete cyclic material model, the method combines hexahedral and beam-column finite elements, where the coupling between them is achieved through kinematic constraints. The kinematic constraints are enforced at each hexahedral node, located at the interface between the beam and the solid elements, as follows:

$$\underset{(3x1)}{\boldsymbol{u}_i^{HEXA}} = \underset{(3x6)}{\boldsymbol{T}_{im}} \cdot \underset{(6x1)}{\boldsymbol{u}_m^{NBCFB}} \tag{4}$$

$$\underset{(3x6)}{\boldsymbol{T}_{im}} = \begin{bmatrix} 1 & 0 & 0 & 0 & z_i - z_m & y_m - y_i \\ 0 & 1 & 0 & z_m - z_i & 0 & x_i - x_m \\ 0 & 0 & 1 & y_i - y_m & x_m - x_i & 0 \end{bmatrix} \tag{5}$$

where $\boldsymbol{u}_m^{NBCFB}$ and $\boldsymbol{u}_i^{HEXA}$ are the displacement vectors of the beam-column FE node corresponding to 6 dofs and the hexahedral nodes (3 dof per node) located at the interface, respectively. The subscript *i* of the global coordinates x, y and z, refers to the hexahedral node ID which is located at the interface section $\boldsymbol{\Omega}_i^1$, while subscript *m* refers to the beam-column elemental node ID that controls the displacements (master node) of the interface section $\boldsymbol{\Omega}_i^1$ (Fig. 5). The matrix $\boldsymbol{T}_{im}$, is computed from the compatibility conditions of beam-column and hexahedral nodal Cartesian coordinates.

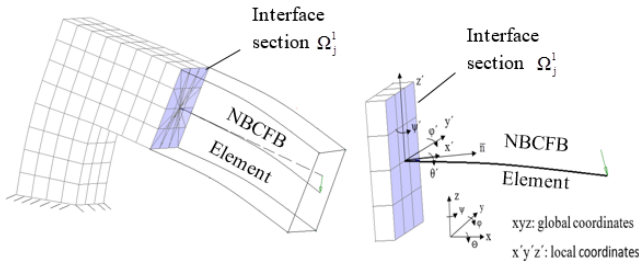

Fig. 5 Kinematic constraints imposed by the 1D structural member on the interface section.

If we assume that a hexahedral node is located at the interface of a beam-column and hexahedral elements, it should follow the body movements of section $\boldsymbol{\Omega}_i^1$, which are enforced by the beam-column element nodal translational and rotational displacements (Fig. 5). Therefore, the computation of the new position for any point on the interface section $\boldsymbol{\Omega}_i^1$ is performed through a linear transformation that is expressed in Eq. (6).

$$\underset{(24x1)}{\boldsymbol{U}^{\text{HEXA}}} = \underset{(24x18)}{\boldsymbol{T}_H} \cdot \underset{(18x1)}{\boldsymbol{U}^{hybrid}} \tag{6}$$

IV. 4-Storey RC Specimen

The SERFIN project [24] was design as such in an attempt to study a full-scale RC multi-storey building under cyclic loading. One of the main objectives of this experiment was to investigate the mechanical behavior of the building and assess the overall mechanical response of the RC frame that was retrofitted with RC infill walls and CFRP jacketing. The 4-storey RC building was tested through the use of the pseudo-dynamic method (PSD) and foresaw two 4-storey parallel frames connected through a continues 0.15 m slab and four out-of-plane central beams that connected the two frames between them (Fig. 6). Each frame consisted of 3 bays (8.9 m

Fig. 6 RC specimen in the lab. [31]

of total span) with the central bay (2.1 m net span) infilled with a RC wall. The total height of the structure was 12 m and the perpendicular distance between the South and North frames was 6.25 m.

According to the experimental setup, the concrete material used for the construction of the RC frame was a C20/25 for all structural members, which had a uniaxial compressive strength of $f_c = 20\ MPa$ and a Young Modulus of elasticity $E_c = 30\ GPa$ with a unit weight of 25 kN/m^3. Two steel grades were used to construct the reinforcement of the frame with a 400 and 450 MPa yielding stress, respectively.

In regards to the loading histories that were chosen to be applied on the structure, the experiment foresaw three different loading sets that corresponded to three independent earthquake intensity levels. The first displacement history shown in Fig. 7, which resulted from the first load set, was scaled accordingly in order to represent a low seismic acceleration of 0.1g, while the second was computed by using a high acceleration equal to 0.25g. The final loading set was developed in order to push the specimen to its ultimate carrying capacity. In this work, the developed FE model was used to simulate the first displacement history of the experiment (Fig. 7).

Fig. 7 Displacement history applied at the top floor of the specimen.

V. Finite Element Mesh

This section will briefly present the HYMOD FE mesh that was developed for the needs of the analysis performed in this research work. As it can be seen in Fig. 8, the 3D detailed full hexahedral FE mesh is shown, which consists of 16,662 hexahedrons according to Table 1 (excluding the CFRP jacketing) and 31,246 embedded rebar elements. This model discretizes the exact geometry of the 4-storey RC specimen, while the embedded rebar elements were modeled based on the exact steel reinforcement geometry (Fig. 8) according to the rebar details reported in [24]. The Full Hexa model was found

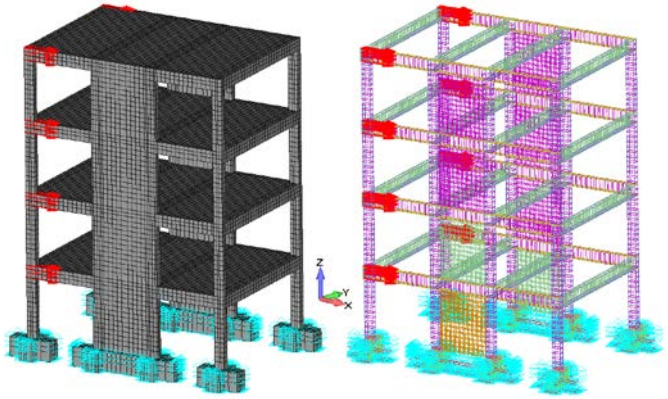

Fig. 8 Full Hexa FE mesh. (Left) Discretization of the concrete domain and (Right) Embedded rebar elements.

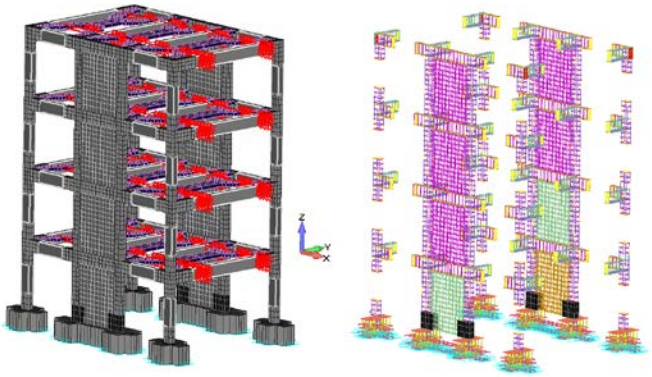

Fig. 9 HYMOD FE mesh. (Left) Discretization of the concrete domain and (Right) Embedded rebar elements.

	Model	Hexa Elements	Rebar Elements	RC Beam Elements	
1	Full Hexa	16,662	31,246	-	
2	HYMOD	8,356	20,646	48	
	Model	Hexa FE Reduction (%)	Rebar FE Reduction (%)	Overall FE Reduction (%)	Dofs Reduction (%)
1	Full Hexa	-	-	-	-
2	HYMOD	49.85	33.92	39.46	48.47

Table 1 FE mesh details of the 4-storey RC frame models.

to have a very high computational demand that made it impossible to be used for the full nonlinear cyclic analysis. Thus the construction of the HYMOD mesh was performed by applying a reduction level 1 (for additional details regarding reduction levels see [8]) that foresaw the deletion of all hexahedral elements found at beam and column structural members, as illustrated in Fig. 9. The derived HYMOD mesh presented in Fig. 9, where the concrete and reinforcement FE can be seen, derived a decrease of the initial number of elements by 39.46% and a total decrease of 48.47% in the case of the degrees of freedom (Table 1).

As it can be depicted from Figs 9 and 10, the plastic hinge length that was adopted was based on the recommendations found in [8], which foresee a range between *h* and *2h*, where *h* is the height of the structural member's section.

The imposed displacement history was applied through kinematic constraints at the nodes of the four slabs that were located at the points of the actuator attachment beams-slab connections as can be seen in Fig. 10 (for the case of the roof slab). The displacement history that was applied on each slab during the analysis, were based on the displacements reported in [24].

It must be noted at this point that, the experiment [24] foresaw the application of forces at each slab, whereas the response of the structure was monitored. The experimentally derived displacements at each slab were applied within the numerical model shown in Figs 9 and 10, where the numerically predicted base shear for each displacement increment were compared with the corresponding experimental values.

VI. Analysis Results

The imposed cyclic loading (Fig. 7) was developed in order to represent a low intensity earthquake excitation of a 0.1g seismic acceleration. As it was reported in [31], during the test the structure developed hairline cracks that appeared on the surface of the wall that were eventually closed down when the first cyclic loading history was finished. This implies that the structure entered the nonlinear state from the very first set of displacement cycles, thus concrete had developed cracks at an early loading stage. The maximum horizontal displacement at the roof according to the experimentally obtained displacement history was 23.5 mm along the positive x-axis and 23 mm along the negative.

Fig. 11 illustrates the von Mises strain contour for the case of the maximum negative horizontal displacement of the top floor (δ_H = -23 mm). It is easy to observe that the South frame develops larger strains at the area of the wall in comparison to the North wall, given that the foreseen reinforcement ratio was lower in the case of the South infill RC wall. The main strain concentrations were found to be located at the walls and joints of the structure, where the bending moments and shear forces were larger. In addition to that, the joints where the beams are

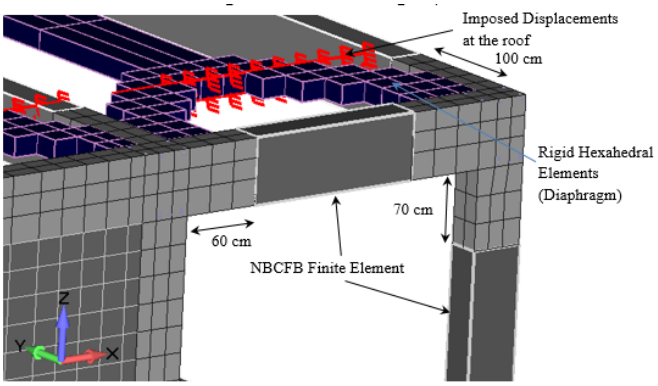

Fig. 10 Geometrical details of the plastic hinge lengths and imposed displacements.

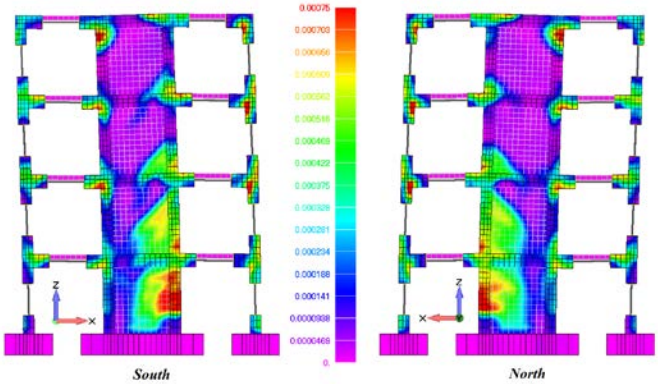

Fig. 11 Von Mises strain contour for δ_H = -23 mm details of the plastic hinge lengths and imposed displacements.

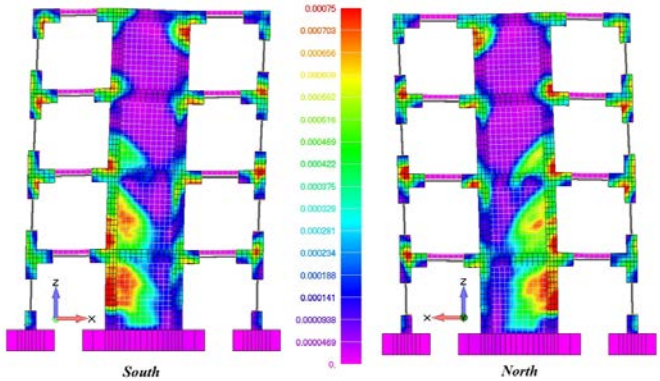

Fig. 12 Von Mises strain contour for δ_H = 23.5 mm details of the plastic hinge lengths and imposed displacements.

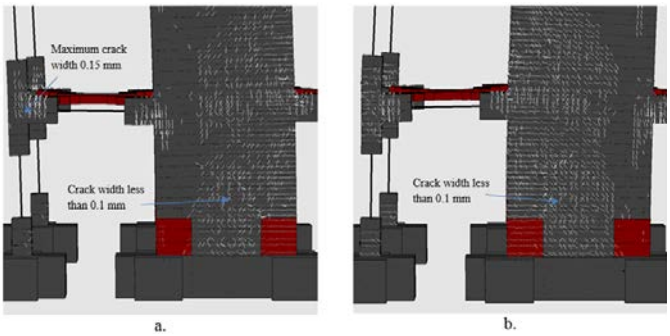

Fig. 13 Crack pattern of the South wall for (a) δ_H = -23 mm and (b) δ_H = 23.5 mm. Maximum computed crack width 0.15 mm.

connected with the walls are also illustrating strain concentrations (Fig. 11), where the contour indicates diagonal cracking in the middle of the wall. The cracks that were computed were small (0.15mm crack thickness at the first floor beam-column joints and 0.1 mm at the shear wall's web). Fig. 12 shows the corresponding von Mises strain contour for the case of δ_H = 23.5 mm, where the maximum positive horizontal displacement was applied. As it can be easily observed, the South wall derived higher strains due to the pre-mentioned reason (weaker wall due to a lower reinforcement ratio). According to their experimental observations, Martin et. al [24] reported that the walls developed diagonal cracks that closed after the load test was completed, which complies with the numerical findings. The numerically computed crack pattern for the case of the two maximum horizontal displacements (negative and positive) can be seen in Figs. 13a and 13b. In addition to that, the opening and closing of cracks can be easily depicted from these two figures, highlighting the numerical ability of the crack opening-closing algorithm that was proposed in [6] to handle this complex phenomenon.

The remaining strain contour that derived, after the 1st load test analysis was fully applied, can be seen in Fig. 14, where it is easy to observe that the remaining strains are very small ($3x10^{-4}$). Based on the numerical analysis, the walls and joints were the areas of the structure that developed the highest deformations (concrete was damaged but the steel remained in the elastic region). The cyclic analysis revealed that the South wall developed higher values, in terms of strains, compared to the North wall (due to the difference in the reinforcement ratio). It was also numerically found that the areas where the CFRP jacketing was applied managed to maintain a low stress-strain state due to the locally induced confinement.

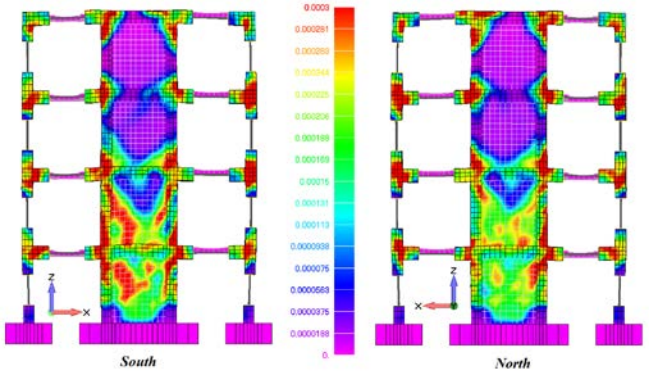

Fig. 14 Remaining von Mises strain contour after the completion of the 0.1g test.

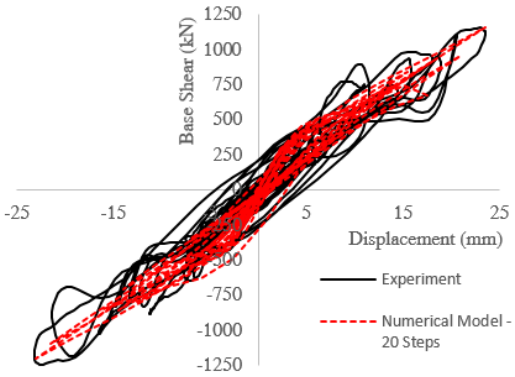

Fig. 15 Experimental vs numerical curves. Total base shear-horizontal displacement of the top floor.

Fig. 15 shows the comparison between the numerical and experimental base shear-horizontal displacement curves, where it can be seen that the hysteretic loops of the experimental curve are slightly larger than the corresponding numerical, especially at the maximum and minimum points of the experimental curves. This is attributed to the fact that the numerical model does not take into account the effect that time (duration of each applied displacement) has on the RC frame's mechanical response. As it resulted from the experimental data, the corresponding hysteretic loops of the curve illustrate vertical parts at the two ends of each loop, where the displacement reaches its maximum value and the RC frame is found to be at an un-loading state. The actual duration that the structure was pushed for with a positive 23.5 mm or a negative 23 mm horizontal displacement can increase the damage induced in the concrete material and also affect the measured structural response in terms of resistance.

The maximum positive and negative numerically predicted total base shears are found to agree with the experimental values in a satisfactory way. For the positive maximum cycle, the numerical results predicted a 1,160 kN, while the corresponding experimental value was 1,152 kN (0.7% difference). For the case of the maximum negative deformation the difference was 3% in favor of safety. It is evident that the HYMOD managed to capture the maximum experimental base shear with high accuracy for this first loading test.

Table 2 shows the computational time that was required for the solution of this problem that foresaw a total of 450 displacement increments and a total of 2,833 internal iterations. The solution of the entire numerical problem required a total of 15 hours and 30 minutes, which corresponds to a 19.7 seconds per internal iteration. The average internal iterations per displacement increment was 6.3, whereas the average numerical error was found to be equal to 1.01×10^{-5}.

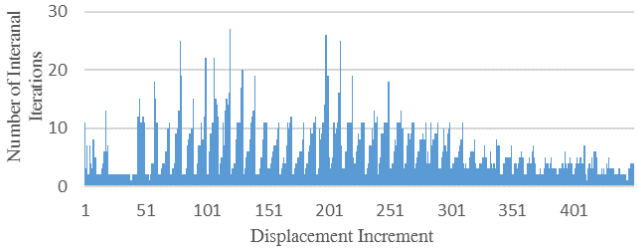

Fig. 16 Number of internal iterations vs displacement increment.

Number of Displ. Incr. per loading cycle	Total Displ Incr. Solved	Total Internal Iter. Solved	Average Numerical Error	CPU Time Nonlinear Solution (hours)	Size of the Output File (Gb)
20	450	2,833	1.01×10^{-5}	15.5	20.7

Table. 2 Computational performance of the HYMOD algorithm for the case of the 0.1g test.

The total required disk space in order to save the output file was 20.7 Gb, which underlines the significance of the HYMOD approach and the ability to efficiently solve such a problem almost 2,833 times. It must be noted here that a 3.7 GHz core was used to perform the numerical computations.

As it was mentioned in [6] and as it is verified through this work, the proposed cyclic material model illustrates stability thus the number of the required iterations to achieve convergence is small, minimizing the computational demand during the nonlinear analysis. This was also verified herein, as it can be seen in Fig. 16 that visualizes the number of internal iterations per displacement increment. According to the statistical analysis performed on this graph, it was found that 47.11% (212) of the displacement increments require less than 5 internal iterations to reach convergence, while 77.33% (348) require less than 10. Finally, only 1.55% (7) of the displacement increments required more than 20 internal iterations so as to achieve convergence, which demonstrates the robustness and numerical stability of the developed algorithm. Furthermore, the use of the beam-column finite element that was described in [8], induces additional stability to the overall performance of the cyclic nonlinear solution, which was found to converge faster not only due to the decrease of the number of solid elements, but due to the numerical stability incorporated by the 1D element that uses the force-method. The numerical investigation performed herein, revealed that a similar numerical behavior derives during the cyclic analysis, thus the algorithmic and numerical benefits of the HYMOD apply for both monotonic [8] and cyclic nonlinear analyses. It must be stated here that, the nonlinear solver used an energy convergence criterion that foresaw a tolerance of 10-5.

Finally, an analysis was also performed through the use of the Full Hexa mesh (Fig. 8) for a single load increment in order to compare the computational demand with that of the HYMOD. The Full Hexa model required a total of 39.83 minutes so as to solve 8 internal iterations, which corresponds to a 298.75 seconds per internal iteration. This constitutes that the HYMOD was found to be 15 times faster than the corresponding Full Hexa model, while in order to solve the 2,833 internal iterations that were presented in Table 2, the Full Hexa model would require a total of 9.8 days given that the installed RAM was sufficient and the analysis would have been feasible. This highlights the importance of the implemented HYMOD approach when it comes to solving large-scale numerical models.

VII. Conclusion

A numerical investigation was performed and presented through this research work that dealt with the full-scale nonlinear cyclic modeling of a 4-storey RC building that was retrofitted with RC infill walls and CFRP jacketing. The experimental setup was modeled and analyzed through the use of the HYMOD approach for cyclic modeling, which foresees the use of 3D detailed FE mesh discretization of the shear-dominated parts of the structure, while the rest of the structural members are modeled through the computationally efficient NBCFB element.

After the solution of the full unreduced hexahedral model for a single load increment, it was found that the required computational time for the simulation of the 4-storey RC building was 15 times slower, whereas the HYMOD approach managed to increase the computational efficiency of the simulation by 1500%. This is attributed to the fact that when the full model is considered the large-scale numerical problem derives a stiffness matrix that requires significant computational demand in order to be updated and inversed during the nonlinear solution procedure. This demonstrates the numerical ability of the HYMOD approach to decrease the stiffness matrix considerably, without losing its corresponding modeling accuracy, providing with the ability to simulate for the entire cyclic displacement history test in an affordable computational time.

The numerical investigation revealed that the adopted HYMOD mesh managed to capture in a realistic manner the experimental shear base results [24] that were applied during the 0.1g loading test with less than 3% deviation. This highlights the ability of the HYMOD algorithm in predicting the overall mechanical behavior of full-scales structures under cyclic loading conditions. Based on the obtained numerical results, the crack pattern, the maximum crack width and the computed base shears were found to be in a good agreement with the experimental data. Furthermore, the ability of the algorithm to maintain a low ratio of internal iterations per displacement increment demonstrates the numerical robustness when using HYMOD in cyclic nonlinear limit state analyses.

Finally, the 0.25g and funeral loading histories are currently being investigated through the use of the same model and will be discussed in a future publication. One of the main numerical challenge that is encountered in the case of these two loading histories is related on how to numerically account for the material deterioration of concrete that already occurred during the 0.1g and 0.25g tests, when analyzing the frame for the case of the funeral loading set. Performing the full analysis for all three loading histories would be computationally extremely demanding, thus solving this numerical problem requires a different approach that will lead to realistic models and numerical results.

Acknowledgment

The author would like to acknowledge the financial support of the Universitad Catholica de la Santisima Concepcion for the needs of this research project through internal funding.

References

[1] H. Hartl, "Development of a continuum mechanics based tool for 3D FEA of RC Structures and application to problems of soil structure interaction." Ph.D. thesis, Faculty of Civil Engineering, Graz Univ. of Technology, 2002.

[2] G.Ch. Lykidis, and K.V. Spiliopoulos, "3D solid finite element analysis of cyclically loaded RC structures allowing embedded reinforcement

slippage", Journal of Structural Engineering-ASCE, 2008,134(4), pp. 629-638.
[3] J. Červenka and V.K. Papanikolaou, "Three dimensional combined fracture-plastic material model for concrete", International Journal of Plasticity, 2008, 24(12), pp. 2192-2220.
[4] V.K. Papanikolaou and A.J Kappos, "Numerical study of confinement effectiveness in solid and hollow reinforced concrete bridge piers: Part 1: Methodology and Part 2: Analysis results and discussion. Engineering Structures", 2009, Vol. 87, pp. 1427–1439, pp. 1440-1450.
[5] G. Markou and M. Papadrakakis, "Computationally efficient 3D finite element modeling of RC structures", Computers and Concrete, 2013, 12(4), 443–98.
[6] Ch. Mourlas, M. Papadrakakis and G. Markou, "A computationally efficient model for the cyclic behavior of reinforced concrete structural members", Engineering Structures, 2017, Vol. 141, pp. 97-125.
[7] H. Bark, G. Markou, Ch. Mourlas and M. Papadrakakis, "Seismic Assessment of a 5-Storey Retrofitted RC Building", *ECCOMAS Congress, VII European Congress on Computational Methods in Applied Sciences and Engineering*, Crete Island, Greece, 5–10 June 2016.
[8] G. Markou and M. Papadrakakis, "A Simplified and Efficient Hybrid Finite Element Model (HYMOD) for Non-Linear 3D Simulation of RC Structures", Engineering Computations, 2015, Vol. 32 (5), pp. 1477-1524.
[9] L. Formaggia, J.F. Gerbeau, F. Nobile and A. Quarteroni, "On the coupling of 3D and 1D Navier–Stokes equations for flow problems in compliant vessels", Computational Methods in Applied Mechanics and Engineering, 2001, Vol. 191, pp. 561:582.
[10] S.A. Urquiza, P.J. Blanco, M.J. Venere, and R.A. Feijoo, "Multidimensional modelling for the carotid artery blood flow", Computational Methods in Applied Mechanics and Engineering, 2006, Vol. 195, pp. 4002:4017.
[11] P.J. Blanco, R.A. Feijoo, and S.A. Urquiza, "A unified variational approach for coupling 3D–1D models and its blood flow applications", Computational Methods in Applied Mechanics and Engineering, 2007, Vol. 196, pp. 4391:4410.
[12] J. Huang, "Numerical solution of the elastic body-plate problem by nonoverlapping domain decomposition type techniques", Math. Comput., 2004, Vol. 73, pp. 19:34.
[13] S.A. Nazarov, "Junctions of singularly degenerating domains with different limit dimensions I", J. Math. Sci., 1996, Vol. 80, pp. 1989:2034.
[14] S.A. Nazarov, "Junctions of singularly degenerating domains with different limit dimensions II", J. Math. Sci., 1999, Vol. 97, pp. 4085:4108.
[15] V.A. Kozlov, and V.A. Maz'ya, "Fields in non-degenerate 1D–3D elastic multi-structures", Quart. J. Mech. Appl. Math., 2001, Vol. 54, pp. 177:212.
[16] L. Formaggia, J.F. Gerbeau, F. Nobile and A. Quarteroni, "On the coupling of 3D and 1D Navier–Stokes equations for flow problems in compliant vessels", Computational Methods in Applied Mechanics and Engineering, 2001, Vol. 191, pp. 561:582.
[17] S.A. Urquiza, P.J. Blanco, M.J. Venere and R.A. Feijoo, "Multidimensional modelling for the carotid artery blood flow", Computational Methods in Applied Mechanics and Engineering, 2006, Vol. 195, pp. 4002:4017.
[18] P.J. Blanco, R.A. Feijoo and S.A. Urquiza, "A variational approach for coupling kinematically incompatible structural models", Computational Methods in Applied Mechanics and Engineering, 2008, Vol. 197, pp. 1577:1602.
[19] P. Mata, A.H. Barbat and S. Oller, "Two-scale approach for the nonlinear dynamic analysis of RC structures with local non-prismatic parts", 2008, Vol. 30(12), pp. 3667:3680.
[20] S. Bournival, J.-C. Cuillière and V. François, "A mesh-based method for coupling 1D and 3D elements." Advances in Engineering Software, 2010, Vol. 41, pp. 838:858.
[21] F. Brezzi, and M. Fortin, Mixed and Hybrid Finite Element Methods, Springer Verlag, 1991.
[22] M. Fortin and A.S. Mounim, "Mixed and Hybrid Finite Element Methods for Convection-Diffusion Problems and Their Relationships with Finite Volume: The Multi-Dimensional Case", Journal of Mathematics Research, 2017, Vol 9(1), pp.68-83.
[23] Reconan FEA v1.00, Finite Element Analysis Software Manual, 2010.
[24] P. Martin, T. Fabio, M.R. Javier, Ch. Christis, K. Nicholas, O. Toula, R. Panayiotis, K. Panagiotis, P. Telemachos, K. Antonis, Seismic Retrofitting of RC Frames with RC Infilling (SERFIN Project), European Commission, Joint Research Center, Institute of the Protection and Security of Citizens, 2013.
[25] M.D. Kotsovos and M.N. Pavlovic, Structural concrete. Finite Element Analysis for Limit State Design, Thomas Telford, London, 1995.
[26] Y.M. Rashid, "Ultimate strength analysis of prestressed concrete vessels", Nucl Eng and Des, 1968, Vol. 7, pp. 334-344.
[27] F. Gonzalez-Vidosa, M.D. Kotsovos and M.N. Pavlovic, "A three-dimensional nonlinear finite-element model for structural concrete. Part 1: main features and objectivity study; and Part 2: generality study", Proceedings of the Institution of Civil Engineers, Part 2, Research and Theory, 1991, Vol. 91, pp. 517-544.
[28] K.J. Willam and E.P. Warnke,, Constitutive model for the triaxial behaviour of concrete, Seminar on concrete structures subjected to triaxial stresses, Instituto Sperimentale Modeli e Strutture, Bergamo, Paper III-1, 1974.
[29] M. Menegotto, and P.E. Pinto, "Method of analysis for cyclically loaded reinforced concrete plane frames including changes in geometry and non-elastic behavior of elements under combined normal force and bending." *Proceedings, IABSE Symposium on Resistance and Ultimate Deformability of Structures Acted on by Well Defined Repeated Loads*, Lisbon, Portugal, 15–22, 1973.
[30] G. Markou and M. AlHamaydeh, "3D Finite Element Modeling of GFRP-Reinforced Concrete Deep Beams without Shear Reinforcement", International Journal of Computational Methods, International Journal of Computational Methods, 2017, 15(1), pp. 1-35.
[31] N. Kyriakides, Ch.Z. Chrysostomou, P. Kotronis, E. Georgiou and P. Roussis, "Numerical simulation of the experimental results of a RC frame retrofitted with RC Infill walls", Earthquakes and Structures, 2015, vol. 9 (4), pp. 735-752.